



Study of residue patterns of aqueous nanofluid droplets with different particle sizes and concentrations on different substrates



H.H. Lee^a, S.C. Fu^a, C.Y. Tso^{a,b}, Christopher Y.H. Chao^{a,*}

^aDepartment of Mechanical and Aerospace Engineering, The Hong Kong University of Science and Technology (HKUST), Hong Kong

^bHKUST Jockey Club Institute for Advanced Study, The Hong Kong University of Science and Technology (HKUST), Hong Kong

ARTICLE INFO

Article history:

Received 12 April 2016

Received in revised form 19 September 2016

Accepted 19 September 2016

Keywords:

Droplet
Evaporation
Nanofluid
Residue pattern

ABSTRACT

Nanofluid droplet evaporation has attracted great interest due to its applications such as in painting, coating and patterning. In most studies, either the particle size or the concentration of nanofluid is considered as a factor in the formation of the residue pattern. This work aims to investigate the effect of both particle size and concentration on the residue pattern. A comprehensive study was made of the residue patterns of Al₂O₃ and TiO₂ aqueous nanofluid droplets on different substrates (i.e. glass, stainless steel and Teflon). It was found that a ring-shaped pattern was formed at low concentrations and small particle sizes, while a uniform pattern was formed at high concentrations and large particle sizes for Al₂O₃ nanofluids. In addition, only ring-shaped residue patterns were observed for all concentrations of TiO₂ nanofluids. In the case of different substrates, on a material with a high contact angle with water, it was difficult to form a ring-shaped pattern. The widths of the ring-shaped pattern were analyzed as well. The results showed that the width of the ring-shaped pattern was larger for small particles. The materials of substrate and nanoparticle also influenced the width.

© 2016 Published by Elsevier Ltd.

1. Introduction

The evaporation of a colloidal droplet and the formation of the residue pattern are crucial to many applications as such inkjet printing [1], virus detection [2], DNA stretching [3–5] and colloidal self-assembly [6–8]. The size of particle can alter its movement inside the droplet [2,9,10]. Small particles tend to approach the three-phase contact line of the droplet and form ring-shaped patterns while large particles appear closer to the center in the residue. Hence, this results in different residue patterns for different particle sizes. This influences the performance of the applications. For example, the size of pigment particles inside a commercial ink product for printing ranges from tens to hundreds of nanometers [1]. Bermel et al. [1] found that using a smaller particle size pigment could improve the printed image quality without losing the lightfastness by reducing the particle size less than 50 nm. However, it is easier for small particles in a droplet to move to the contact line. This causes poor performance due to the uneven distribution of pigment and formation of ring-shaped patterns. Therefore, the suppression of the ring-shaped residue pattern is

necessary in inkjet printing. The residue pattern depends on the particle size, evaporation dynamics, concentration of fluid, material of substrate and material of nanoparticle, etc.

Some factors of drying patterns of a colloidal droplet have been investigated. For instance, Monteux and Lequeux [11] found that nanoparticles segregated at the edge of the drop of a polydispersed nanometric and micrometric particles colloidal suspension. They suggested nanoparticles had a different packing behavior to form patterns from microparticles. Adding surfactant into nanofluid is a common practice for the stability. However, adding surfactant influences the residue pattern. Crivoi and Duan [12] investigated the effect of surfactant on drying patterns. Adding Cetyltrimethylammonium Bromide (CTAB) surfactant into graphite nanofluid can help the formation of ring-shaped pattern instead of uniform pattern. The effect of different surfactant, sodium dodecyl sulfate (SDS), was investigated by Still et al. [13] and they found addition of SDS caused a significantly more uniform pattern from drying of polystyrene colloidal suspension. Yunker et al. [14] studied the shaped of the particle in colloid to control the deposition pattern. Ellipsoidal particles uniformly deposited during evaporation. However, Dugyala and Basavaraj [15] investigated the patterns with different shapes of the particle and pH value of the fluid. The result revealed that the particle–particle and particle–surface interaction was more important than the aspect ratio of ellipsoidal particle to control the ring-shaped pattern. Lin et al. [16] found the effect of

* Corresponding author at: Department of Mechanical and Aerospace Engineering, Main Academic Building, The Hong Kong University of Science and Technology, Clear Water Bay, Kowloon, Hong Kong.

E-mail address: meyhchao@ust.hk (C.Y.H. Chao).

Nomenclature

c_1	empirical parameter	w	width of ring-shaped pattern [m]
c_2	empirical parameter		
CCA	constant contact angle [–]	<i>Greek symbol</i>	
CCR	constant contact radius [–]	ϕ	concentration of nanofluid [vol%]
r	radius of the ring-shaped patterns [m]		

the surface hydrophobicity on the patterns of silica nanofluids. The surface with higher surface energy could result in smaller width of ring because the nanoparticles were more readily to move to the contact line.

Some researchers have studied the influence of the nanoparticle size and concentration in nanofluids on droplet residue patterns. With regard to particle size, Chon et al. [17] studied the effect of nanoparticle size and number density on the evaporation and dry out characteristics of strongly pinned nanofluid droplets. Four types of nanofluids were tested experimentally, namely 2 nm Au, 30 nm CuO, 11 nm Al₂O₃, and 47 nm Al₂O₃ at 0.5 vol%. A nanofluid droplet was put on a micro-heater array under a constant voltage mode. They found that smaller nanoparticles had a wider edge and more central deposition while larger nanoparticles resulted in narrower stains at the edge with a less central deposition. In other words, larger particles were likely to form a ring-shaped pattern because larger particles have a higher number density of particles, leading to a lower viscosity of the fluid. Wong et al. [2] investigated the sizes of particle separation, which is caused by different traveled distances of the various particle sizes during droplet evaporation. Carboxylate-modified negatively charged-stabilized fluorescent polystyrene spheres with diameters of 40 nm, 1 μ m and 2 μ m prepared in deionized water were used in their experiment. Suspension droplets on a pre-cleaned glass substrate underwent evaporation under ambient conditions. Three well-separated rings were observed on the substrate after evaporation. The outermost rings and the innermost rings were formed by 40 nm and 2 μ m particle suspensions, respectively. Similar results were found for using amine-modified positively charge-stabilized particles. The smaller particles moved closer to the contact line whereas the larger particles moved closer to the center. The result is not the same as that of Chon et al. [17] and it is believed that apart from particle size, other factors may also affect the residue pattern.

Regarding the concentrations, a series of experiments were conducted by Sefiane [18]. Aqueous nanofluids with Al₂O₃ nanoparticles with diameters smaller than 100 nm were examined and a Teflon surface was used as the substrate. The effect of concentration (0.1%, 0.5%, 1% and 2%) on the residue patterns was studied. It was found that all nanofluids formed ring-shaped patterns and the thickness of the rings increased with the concentration so that the increase of concentration was approximately proportional to the increase of the thickness of the ring. Jing and Ma [19] studied a 75 nm silica aqueous nanofluid from 20 wt% to 53 wt% evaporations and patterns experimentally. The result showed that the average radius of the circular cracks, which are cracks inside the residue pattern, decreased with increasing the concentration of nanofluid. While the average distance between two adjacent circular cracks increased with the increasing concentration of nanofluid. Therefore, the patterns are dependent on the concentration of the nanofluid. Brutin [20] studied the patterns of a nanofluid with 24 nm diameter particles whose density was equal to water, with 0.01–5.7% concentrations. It was observed that from 0.01% to 0.47%, ring-shaped patterns were formed and the width of the ring increased with the concentration. For the concentrations of 1.15% and above, axisymmetric flower petal patterns were discovered

and the thicknesses increased with concentration. Also, the width of the ring and the concentration were correlated in the power law. Lebovka et al. [21] studied the effect of the concentration of Laponite-based aqueous nanofluids. It was found the coffee-ring effect only for the initial Laponite concentration less than 1 wt% while dome-like deposition for the Laponite concentration exceeding 1 wt%.

The works mentioned above either focused on the particle concentration or the particle size, but there has been a lack of studies to investigate the combined effect of both. Deegan [22] investigated a 0.1 and 1 μ m sulfate-terminated polystyrene microsphere suspension with 0.063–2 vol% on a mica substrate. It was reported that the 0.1 μ m suspension formed four well-defined ring patterns for the 1 vol% and less organized rings for lower concentrations. For 1 μ m suspension, ring patterns were formed with many arches for all concentrations and the distribution function of the arches shifted to a larger value with decreasing concentrations. In addition, the relation of the width of the ring and the nanofluid concentration was shown in a power law equation. These results show that the residue pattern depends not only on the particle size, but also the concentration. However, only two sizes were considered in Deegan's experiment and the smallest size was 100 nm which cannot represent the case of nanofluids.

The objective of this paper is to systematically investigate the residue patterns of different particle sizes and concentrations of nanofluid and different substrate materials. Nanofluids with Al₂O₃ nanoparticle sizes of 9 nm, 13 nm, 20 nm, 80 nm and 135 nm and with TiO₂ nanoparticle sizes of 21 nm in diameter and 0.01 vol%, 0.05 vol%, 0.1 vol%, 0.5 vol%, 1 vol%, 2 vol%, 3 vol% and 4 vol% on glass, stainless steel and Teflon, respectively, are examined in this work. After the evaporation of the nanofluid droplets, the patterns of the deposited particles were captured by a camera. Since the patterns are influenced by the evaporation dynamics [23], the contact angle and the contact diameter were measured by a goniometer during evaporation. The formation of different residue patterns will be discussed and the patterns will be characterized, including the analysis of the width of the ring-shaped patterns.

2. Materials and experimental set-up

A two-step approach [24–27] was used to prepare the nanofluids. The first step was to synthesize the nanoparticles, and the second step was to disperse the nanoparticles in the base fluid. The benefits of this process are that they are easy to perform and applicable to different types of nanoparticles. However, the nanoparticles may easily become agglomerated with each other, leading to instability of the nanofluids. If the effective size of the particles becomes larger with agglomeration, the characteristics of the nanofluids, e.g. their thermophysical properties are affected. To prevent agglomeration, the nanofluids were put in an ultrasonic bath (Branson 3800, Branson Ultrasonics, US) in the preparation process.

Fig. 1 shows a schematic diagram of the experimental setup for investigating the evaporation kinetics of nanofluids. A droplet, whose volume was controlled at 2.5 μ L by a micro-pipette, was

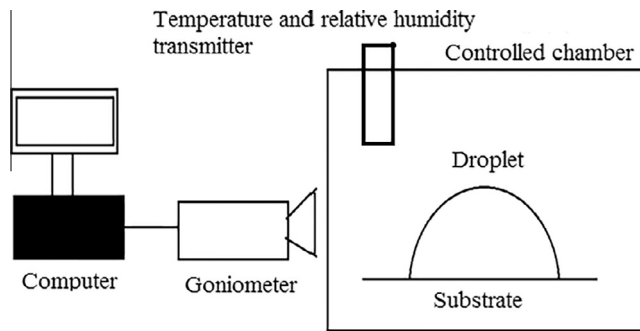


Fig. 1. Schematic diagram of the experiment setup for investigating evaporation kinetics.

placed on a substrate surface in an environmentally controlled chamber. Three materials were chosen for the substrate: glass, stainless steel and Teflon. The temperature was controlled at 25 ± 1 °C and the relative humidity was set at $30 \pm 3\%$ and these were measured by a temperature and humidity transmitter (HMP233, Vaisala, Finland). Commercially available glass, stainless steel and Teflon were used as the substrates. The substrates were cut in size of $75 \text{ mm} \times 45 \text{ mm}$. The experiments and measurements were conducted on an optical table to ensure the substrate was horizontal. The equilibrium contact angles with DI water to the substrates and the roughnesses of the substrate, glass, stainless steel and Teflon are 55.2° , 80.9° and 90.4° and 5.1, 281.5 and 473.2 nm. The contact angles were determined by a contact angle meter (Digidrop, GBX, France) with five repetitions. The roughnesses were measured at 5 different points on the surface using an optical profiler (Wyko NT3300 Profiler, Veeco, US). Before each test, the substrate was cleaned in an ultrasonic bath for half an hour and then cleaned with acetone. The evaporation process was recorded by the contact angle meter. The contact angle and the contact diameter of the droplet were measured every 30 s. The droplet evaporation process can be divided into three modes [28]. One is the constant contact radius (CCR) mode with the contact angle decreasing. The following mode is named the constant contact angle (CCA) mode in which the contact angle is constant and the contact radius decreases. The last mode is the mixed mode in which both the contact angle and contact diameter decrease. It is found that there are all three modes for water on a stainless steel substrate in the evaporation process. The same result was reported by Simon and Hsu [29]. For nanofluids, there is only CCR mode during the evaporation process for all concentrations and particle sizes on all substrate. It is believed that the evaporation dynamics is independent of the substrate for nanofluid.

After evaporation of the droplet, there was a residue pattern on the substrate. The pattern was recorded by a camera connected to a microscope (M205C, Leica Microsystems, Germany). Fig. 2 shows one of the images for the pattern captured by the camera. If the residue was a ring-shaped pattern, the width of the ring was further analyzed by measuring the width and the radius of the ring as illustrated in Fig. 2. The width might not be uniform, so the widths at six different points, points 1–6 as shown in Fig. 2, were measured. The ring width presented were the mean value of them. The experiments were conducted three times to verify the width and the pattern. As an illustrative example, Fig. 3 shows the patterns of the three trials of the experiments of 0.01 vol% 9 nm Al_2O_3 nanofluid.

3. Results and discussion

The residue pattern appeared when the nanofluid droplet had fully evaporated. With different particle sizes and concentrations,

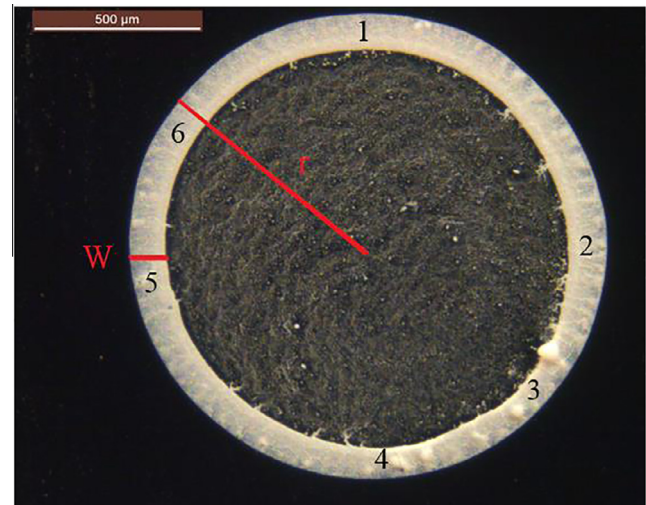


Fig. 2. Ring width and radius of the ring in the pattern. w and r denote the width and the radius. The measurement of the width is performed at points 1–6.

there are different residue patterns. In this study, different concentrations from 0.01 vol% to 4 vol%, and particle sizes from 9 nm to 135 nm in diameter are examined. Three types of pattern are observed: (1) a ring-shaped pattern, (2) a uniform pattern and (3) an irregular pattern. The ring-shaped patterns result from the accumulation of particles at the periphery, forming a ring shape. The uniform patterns represent particles distributed through the whole contact base area including the periphery and center. The irregular patterns are where particles are mainly found in the center and the shape is irregular.

It is observed that the residue patterns depended on both the concentrations and particle sizes. Figs. S1–S5 in the supplementary document show the residue patterns with different sizes and concentrations of Al_2O_3 nanofluids on stainless steel. Figs. S6–S8 are the result of 21 nm TiO_2 nanofluids with different concentrations on glass, stainless steel and Teflon, respectively. The residue patterns of Al_2O_3 nanofluids on glass and Teflon are not shown. Table 1 summarizes the results of the patterns of different nanofluids and substrates. Generally, the ring-shaped patterns are found in the left and top of Table 1. This means small particle size and low concentration Al_2O_3 nanofluids are likely to form ring-shaped patterns. The uniform patterns appear in the right and bottom of Table 1. In other words, there is a tendency for large particle size and high concentration of Al_2O_3 nanofluids to form uniform patterns. Regarding the irregular patterns, these are in the middle of Table 1 and show that moderate particle size and concentration Al_2O_3 nanofluids form irregular patterns. Fig. 4 reveals ring-shaped, irregular and uniform patterns at different particle sizes and concentrations of Al_2O_3 nanofluids. Fig. 4(a) demonstrates the ring-shaped pattern of small particle size and low concentration nanofluid, while Fig. 4(b) shows the irregular pattern of moderate concentration and particle size. Fig. 4(c) illustrates the uniform pattern of high concentration and large particle size.

Therefore, the patterns are determined by both particle size and concentration instead of solely either particle size or concentration. In terms of different materials of nanoparticles, namely Al_2O_3 and TiO_2 , the Al_2O_3 nanofluid forms ring-shaped patterns, irregular patterns and uniform patterns depending on the concentration and substrate material. However, in the case of 21 nm TiO_2 nanofluid, ring-shaped patterns form at all concentrations and substrate materials. This shows that the patterns are also dependent on the materials of the nanofluid particles.

In the case of different substrate materials, the contact angle is a parameter to show the adhesion of a liquid to different solids.

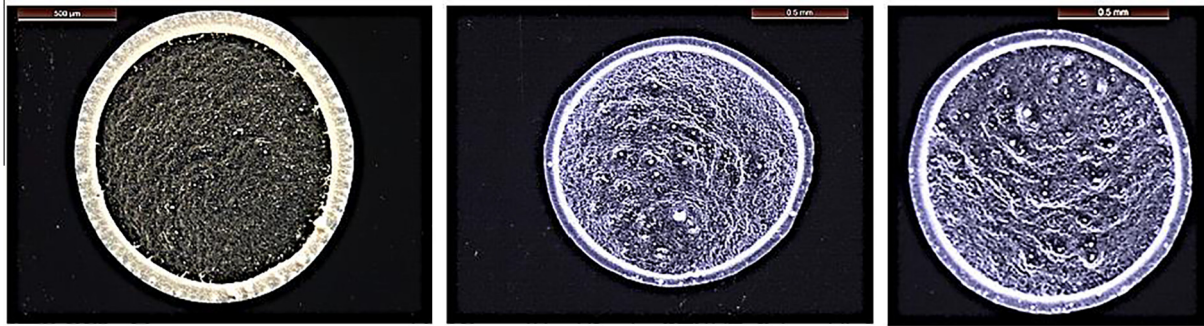


Fig. 3. Patterns of three trials of the experiments of 0.01 vol% 9 nm Al₂O₃ nanofluid.

Table 1

Summary of the residue patterns on different materials of substrates and nanoparticles of Al₂O₃ nanofluid. “G”, “SS” and “T” denote different materials of substrates, glass, stainless steel and Teflon accordingly. For different patterns, “R”, “I”, “U” and “NO” represent ring-shaped, irregular, uniform and not observable, respectively.

		Concentration (vol%)																													
		0.01			0.05			0.1			0.5			1			2			3			4								
		G	SS	T	G	SS	T	G	SS	T	G	SS	T	G	SS	T	G	SS	T	G	SS	T	G	SS	T						
Particle Size (nm)	9	R	R	R	R	R	R	R	R	R	R	R	R	R	R	R	R	R	R	R	R	R	U	U	U	R	U	U	R	U	U
	13	R	R	NO	R	R	NO	R	R	R	R	R	R	R	R	R	R	R	R	R	R	R	U	U	U	R	U	U	R	U	U
	20	R	R	NO	R	R	NO	R	I	I	R	I	I	R	I	I	R	I	I	R	I	I	R	I	I	R	I	I	R	U	U
	80	R	R	R	R	R	R	R	I	R	R	I	R	R	R	U	R	U	U	R	U	U	R	U	U	R	U	U	R	U	U
	135	R	R	NO	R	R	R	R	R	R	R	R	R	R	U	R	U	U	U	U	U	U	U	U	U	U	U	U	U	U	U

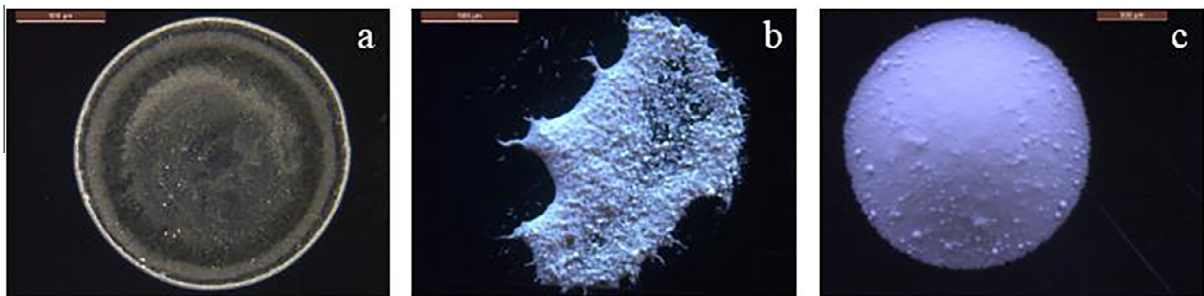


Fig. 4. Comparison of the residue patterns of Al₂O₃ nanofluids in different particle sizes and concentrations (a) 9 nm 0.01 vol%, (b) 80 nm 0.5 vol% and (c) 135 nm 4 vol% on stainless steel. The scale bar is 500 μm.

Three different materials, namely glass, stainless steel and Teflon, were examined in the experiment. These materials are commonly used in daily life and show different wettabilities to water. The measured contact angles of glass, stainless steel and Teflon to water are 55.2°, 80.9° and 90.4°, respectively. Using a comparison from Table 1, the ascending order of the contact angle of water to the substrates, it is found that a substrate with a lower contact angle makes it easier for nanofluids to form ring-shaped patterns. For a substrate with a higher contact angle, for instance, there are less ring-shaped patterns for the stainless steel substrate in high concentrations and large particle sizes than ring-shaped patterns in the same region on the glass. Fig. 5 shows clear illustrations of the comparison of different substrates that more particles remain on the center of the ring on less wettability substrate. This may be attributed to the shape of the droplet being influenced by the contact angle. For a fixed volume of the droplet, a larger contact angle results in larger height and smaller contact diameter as shown in Fig. 5. In the case of a larger contact angle, Fig. 5(b), there are more particles at the center on stainless steel than the particle at the center on glass, in Fig. 5(a). It is because the height of the center is the greatest and an even distribution

of the particles in the nanofluid is presumed due to the ultrasonication before the experiment. Therefore, after the evaporation, there are probably more particles remaining at the center and the patterns become irregular or uniform. In addition, the velocity of the flow in the droplet driven by evaporation is directly proportional to the evaporation rate of the droplet [30]. This flow orients from the center to the periphery of the droplet and contributes to the formation of the ring-shaped patterns. The higher evaporation rate, the higher velocity of the flow. The evaporation rate is directly proportional to the surface area of the droplet. For a fixed volume droplet, the surface area increases with a decreasing contact angle. In other words, a substrate with a lower contact angle results in a larger surface area of the droplet and thus a higher evaporation rate and higher velocity of the flow. It is easier for a substrate with a lower contact angle to form ring-shaped patterns. The trend of width of the ring can also be explained by these reasons. The width of the ring decreases with a decreasing contact angle and this will be discussed in the end of this section.

The effects of number density of the nanofluid and the specific gravity of the nanoparticle on the patterns are reported by Chon et al. [17]. They found that the greater viscosity and specific gravity

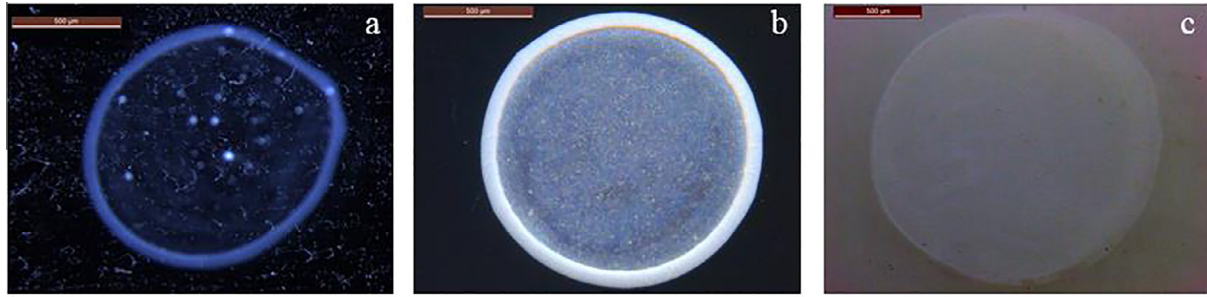


Fig. 5. Comparison of the residue patterns of 0.1 vol% TiO₂ nanofluid on different substrates (a) glass, (b) stainless steel and (c) Teflon. The scale bar is 500 μm.

Table 2
The number density of different concentrations and particle sizes of Al₂O₃ nanofluids on stainless steel.

		Concentration (vol%)							
		0.01	0.05	0.1	0.5	1	2	3	4
Particle Size (nm)	9	2.62E+20	1.31E+21	2.62E+21	1.31E+22	2.62E+22	5.24E+22	7.86E+22	1.05E+23
	13	8.69E+19	4.35E+20	8.69E+20	4.35E+21	8.69E+21	1.74E+22	2.61E+22	3.48E+22
	20	2.39E+19	1.19E+20	2.39E+20	1.19E+21	2.39E+21	4.77E+21	7.16E+21	9.55E+21
	80	3.73E+17	1.87E+18	3.73E+18	1.87E+19	3.73E+19	7.46E+19	1.12E+20	1.49E+20
	135	7.76E+16	3.88E+17	7.76E+17	3.88E+18	7.76E+18	1.55E+19	2.33E+19	3.10E+19

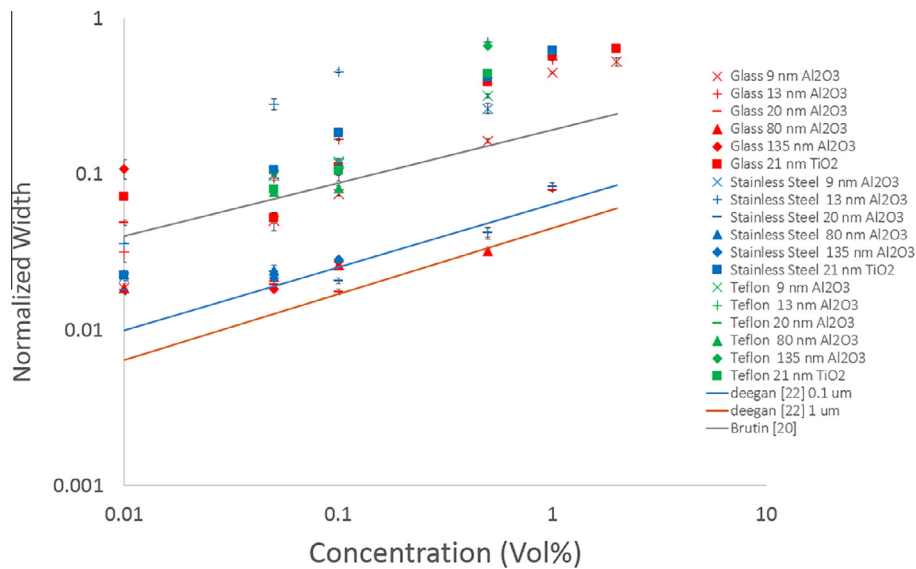


Fig. 6. Normalized ring widths against concentration of different nanofluids.

using different particle materials hinder the particles from moving to the rim of the ring shape. A greater number density results in a greater viscosity in nanofluids [31]. Table 2 gives the number density of the different concentrations and particle sizes of Al₂O₃. For the ring-shaped pattern, the number density of the Al₂O₃ nanofluid ranges from 10¹⁶ to 10²² while the number density of irregular pattern is from 10²¹ to 10²³. With regard to the uniform pattern, the number density is between 10¹⁸ and 10²¹. It is found that the num-

ber density of the uniform pattern is from 10¹⁸ to 10²³. According to this result, it seems that there is no pronounced correlation between the number density and pattern type. The effect of the enhancement of viscosity due to the greater number density is negligible in this case. If the specific gravity and number density are varied simultaneously, as in the work of Chon et al., it is hard to determine which is the factor that hinders the particles in moving to the rim of the ring shape. However, in this study, the specific



Fig. 7. Comparison of the residue patterns of 0.1 vol% Al_2O_3 nanofluid of different particle sizes (a) 9 nm, (b) 13 nm and (c) 135 nm on stainless steel. The scale bar is 500 μm .

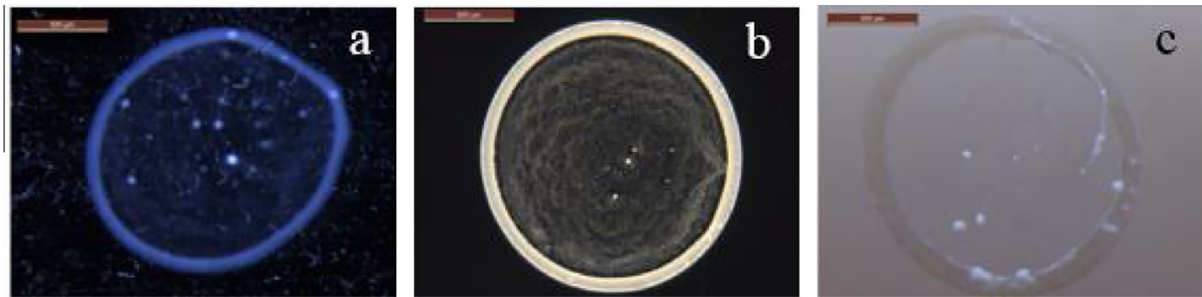


Fig. 8. Comparison of the residue patterns of 0.1 vol% Al_2O_3 nanofluid on different substrates from (a) glass, (b) stainless steel and (c) Teflon. The scale bar is 500 μm .

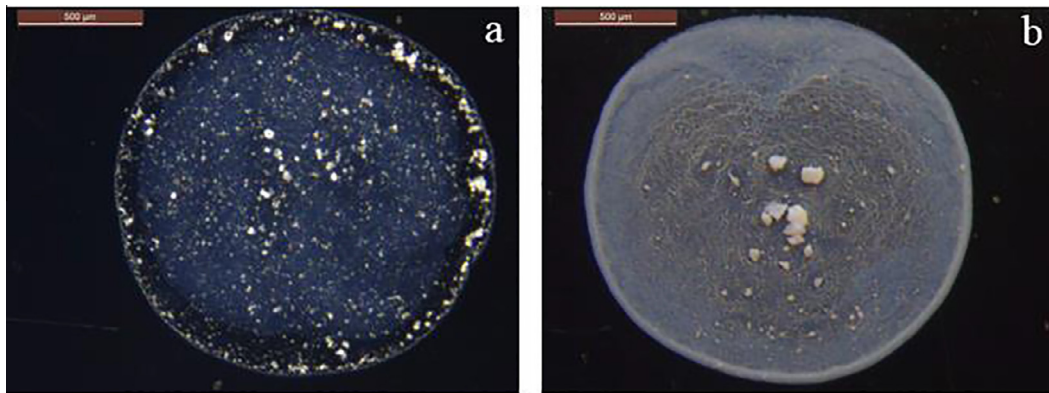


Fig. 9. Comparison of the residue patterns of different materials of nanoparticle (a) Al_2O_3 and (b) TiO_2 in 0.05 vol% nanofluid on stainless steel. The scale bar is 500 μm .

gravity remains unchanged and only the number density is varied. Hence, this can ensure that the number density, instead of the combined number density and concentration, plays an insignificant role in the formation of the patterns.

An analysis of the width of the ring is useful so that the threshold concentration and particle size needed by a nanofluid to form patterns other than ring-shaped patterns can be found. The width of the rings has been studied by researchers [20,22]. Deegan [22] found that the widths of the rings are related to the concentration. He found that

$$\frac{w}{r} = c_1 \phi^{c_2}, \quad (1)$$

where w is the width of the ring [m], r is the radius of the ring-shaped patterns [m], ϕ is the concentration of the nanofluid [vol %], and c_1 and c_2 are the constants. Fig. 2 shows the width of the ring and radius of the ring in the pattern. Deegan conducted the experiment using 0.1 and 1 μm sulfate-terminated polystyrene suspended in a deionized water droplet, sized 0.5 μL , wetting on a mica surface. While Brutin's experimental conditions use different concentrations of nanofluid with the 24 nm, iso-density to water,

carboxylate surface functional group nanoparticles at 50 RH%. Fig. 6 shows the widths of ring patterns against the concentration of different substrate materials and nanofluids. It is found that the normalized widths of small particles are at the top of the figure while those of the large particles are at the lower position in Fig. 6. This means that the small size particle nanofluids tend to form a larger width of the ring-shaped pattern. Fig. 7 shows small particle nanofluids tend to form larger width. In addition, comparing different substrate materials, the less wettability substrate, the greater the width of the ring is shown in Fig. 8. Further, comparing the nanofluids, 21 nm TiO_2 and 20 nm Al_2O_3 , the TiO_2 nanofluid generally forms a greater width of ring than the Al_2O_3 nanofluid in Fig. 9. It is noted that the patterns mainly depend on particle size and concentration. Materials of the substrate and nanoparticle have a less significant effect on the pattern.

4. Conclusions

The residue patterns of Al_2O_3 and TiO_2 aqueous nanofluid droplets were investigated for the effects of different particle sizes and concentrations of nanofluids and various substrates.

An experiment was conducted to observe the residue patterns which were dependent on both particle size and concentration. It was found that a ring-shaped pattern was formed at low concentrations and small particle sizes, below 2 vol% and smaller than 13 nm, while a uniform pattern was formed at high concentrations and larger particle sizes, above or 3 vol% and larger than 20 nm, for Al₂O₃ nanofluid. There were ring-shaped patterns for all concentrations, 0.01–4 vol%, of 21 nm TiO₂ nanofluid. On low wettability substrates, it was hard to form a ring-shaped pattern while on high wettability substrates, it was likely to form a ring-shaped pattern. Regarding the width of the ring, it was found that for small particles, the width of the ring-shaped pattern was larger. Substrate materials with a high contact angle of water showed a greater width. TiO₂ 21 nm nanofluid formed a greater width of ring than that of Al₂O₃ 20 nm nanofluid.

Acknowledgements

Funding sources for this research are provided by the Hong Kong Research Grant Council via General Research Fund account 16201114, Science and Technology Planning Project of Guangdong Province, China, No. 2014B090903007 and Natural Science Foundation of Guangdong Province, China, No. 2015A030310447.

Appendix A. Supplementary data

Supplementary data associated with this article can be found, in the online version, at <http://dx.doi.org/10.1016/j.ijheatmasstransfer.2016.09.093>.

References

- [1] A.D. Bermel, D. Bugner, Particle size effects in pigmented ink jet inks, *J. Imaging Sci. Technol.* 43 (4) (1999) 320–324.
- [2] T. Wong, T. Chen, X. Shen, C. Ho, Nanochromatography driven by the coffee ring effect, *Anal. Chem.* 83 (6) (2011) 1871–1873.
- [3] S. Abramchuk, A. Khokhlov, T. Iwataki, H. Oana, K. Yoshikawa, Direct observation of DNA molecules in a convection flow of a drying droplet, *EPL (Europhys. Lett.)* 55 (2) (2001) 294.
- [4] X. Fang, B. Li, E. Petersen, Y. Seo, V.A. Samuilov, Y. Chen, et al., Drying of DNA droplets, *Langmuir* 22 (14) (2006) 6308–6312.
- [5] I.I. Smalyukh, O.V. Zribi, J.C. Butler, O.D. Lavrentovich, G.C. Wong, Structure and dynamics of liquid crystalline pattern formation in drying droplets of DNA, *Phys. Rev. Lett.* 96 (17) (2006) 177801.
- [6] M.H. Kim, S.H. Im, O.O. Park, Rapid fabrication of Two- and Three-Dimensional colloidal crystal films via confined convective assembly, *Adv. Funct. Mater.* 15 (8) (2005) 1329–1335.
- [7] Z. Lin, S. Granick, Patterns formed by droplet evaporation from a restricted geometry, *J. Am. Chem. Soc.* 127 (9) (2005) 2816–2817.
- [8] J. Xu, J. Xia, S.W. Hong, Z. Lin, F. Qiu, Y. Yang, Self-assembly of gradient concentric rings via solvent evaporation from a capillary bridge, *Phys. Rev. Lett.* 96 (6) (2006) 066104.
- [9] B.M. Weon, J.H. Je, Capillary force repels coffee-ring effect, *Phys. Rev. E* 82 (1) (2010) 015305.
- [10] H. Chang, Y. Chang, Fabrication of Al₂O₃ nanofluid by a plasma arc nanoparticles synthesis system, *J. Mater. Process. Technol.* 207 (1) (2008) 193–199.
- [11] C. Monteux, F. Lequeux, Packing and sorting colloids at the contact line of a drying drop, *Langmuir* 27 (6) (2011) 2917–2922.
- [12] A. Crivoi, F. Duan, Effect of surfactant on the drying patterns of graphite nanofluid droplets, *J. Phys. Chem. B* 117 (19) (2013) 5932–5938.
- [13] T. Still, P.J. Yunker, A.G. Yodh, Surfactant-induced Marangoni eddies alter the coffee-rings of evaporating colloidal drops, *Langmuir* 28 (11) (2012) 4984–4988.
- [14] P.J. Yunker, T. Still, M.A. Lohr, A.G. Yodh, Suppression of the coffee-ring effect by shape-dependent capillary interactions, *Nature* 476 (7360) (2011) 308–311.
- [15] V.R. Dugyala, M.G. Basavaraj, Control over coffee-ring formation in evaporating liquid drops containing ellipsoids, *Langmuir* 30 (29) (2014) 8680–8686.
- [16] S.Y. Lin, K.C. Yang, L.J. Chen, Effect of surface hydrophobicity on critical pinning concentration of nanoparticles to trigger the coffee ring formation during the evaporation process of sessile drops of nanofluids, *J. Phys. Chem. C* 119 (6) (2015) 3050–3059.
- [17] C.H. Chon, S. Paik, J.B. Tipton, K.D. Kihm, Effect of nanoparticle sizes and number densities on the evaporation and dryout characteristics for strongly pinned nanofluid droplets, *Langmuir* 23 (6) (2007) 2953–2960.
- [18] K. Sefiane, On the formation of regular patterns from drying droplets and their potential use for bio-medical applications, *J. Bionic Eng.* 7 (2010) S82–S93.
- [19] G. Jing, J. Ma, Formation of circular crack pattern in deposition self-assembled by drying nanoparticle suspension, *J. Phys. Chem. B* 116 (21) (2012) 6225–6231.
- [20] D. Brutin, Influence of relative humidity and nano-particle concentration on pattern formation and evaporation rate of pinned drying drops of nanofluids, *Colloids Surf., A* 429 (2013) 112–120.
- [21] N.I. Lebovka, V.A. Gigiberiya, O.S. Lytvyn, Y.Y. Tarasevich, I.V. Vodolazskaya, O. P. Bondarenko, Drying of sessile droplets of laponite-based aqueous nanofluids, *Colloids Surf., A* 462 (2014) 52–63.
- [22] R.D. Deegan, Pattern formation in drying drops, *Phys. Rev. E* 61 (1) (2000) 475.
- [23] R.D. Deegan, O. Bakajin, T.F. Dupont, G. Huber, S.R. Nagel, T.A. Witten, Capillary flow as the cause of ring stains from dried liquid drops, *Nature* 389 (6653) (1997) 827–829.
- [24] R. Prasher, D. Song, J. Wang, P. Phelan, Measurements of nanofluid viscosity and its implications for thermal applications, *Appl. Phys. Lett.* 89 (13) (2006) 133108.
- [25] S. Choi, Z. Zhang, W. Yu, F. Lockwood, E. Grulke, Anomalous thermal conductivity enhancement in nanotube suspensions, *Appl. Phys. Lett.* 79 (14) (2001) 2252–2254.
- [26] Y. Xuan, Q. Li, Heat transfer enhancement of nanofluids, *Int. J. Heat Fluid Flow* 21 (1) (2000) 58–64.
- [27] S.K. Das, N. Putra, P. Thiesen, W. Roetzel, Temperature dependence of thermal conductivity enhancement for nanofluids, *J. Heat Transfer* 125 (4) (2003) 567–574.
- [28] R. Picknett, R. Bexon, The evaporation of sessile or pendant drops in still air, *J. Colloid Interface Sci.* 61 (2) (1977) 336–350.
- [29] F. Simon, Y. Hsu, Wetting dynamics of evaporating drops on various surfaces, *NASA TM X-67913* (1971).
- [30] A. Petsi, V. Burganos, Potential flow inside an evaporating cylindrical line, *Phys. Rev. E* 72 (4) (2005) 047301.
- [31] R. Bhardwaj, X. Fang, P. Somasundaran, D. Attinger, Self-assembly of colloidal particles from evaporating droplets: role of DLVO interactions and proposition of a phase diagram, *Langmuir* 26 (11) (2010) 7833–7842.